Virtual Simulation Lab: Simulating a hemisphere with the 3D Virtual Goniometer

Having demostrated the accuracy of VIRGO to compare with an extruded shape using the 2D Virtual Goniometer, we now explore the simulation of a non-extruded shape, namely a 600 mm diameter hemisphere, using the 3D Virtual Goniometer.

In Figure 1, we show a schematic illustration of the 3D VIRGO goniometer. In order to create high resolution 3D polar responses, we are using 13 sources, as specified by ISO 17497-2 and 4,295 receivers, with an angular resolution of 1.6°. The sample is located at the origin of the receiver hemisphere and the sources and receivers at in the far field, at 50m and 10m respectively. The checkerboard base is not involved in the calculation and only shown for contrast.

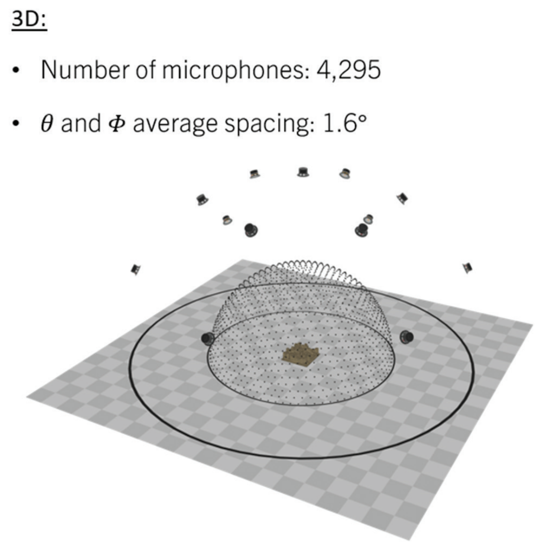

Figure 1. An illustration of the 3D Virtual Goniometer.

In Figure 2, we compare the normal incidence polar responses for 1 hemisphere (a), a linear array of 4x1 hemispheres (b) and a 2x2 grid of hemispheres (c). In Figure 2 (top row), we compare the polar responses of the three samples at 400 Hz. The polar response of the single hemisphere (a) is uniform with no grating lobes, whereas the linear array (b) shows linear spaced grating lobes. The square hemisphere array (c) shows a 2-dimensional pattern. In Figure 2 (bottom row), we compare the polar responses at 2500 Hz. Remembering the

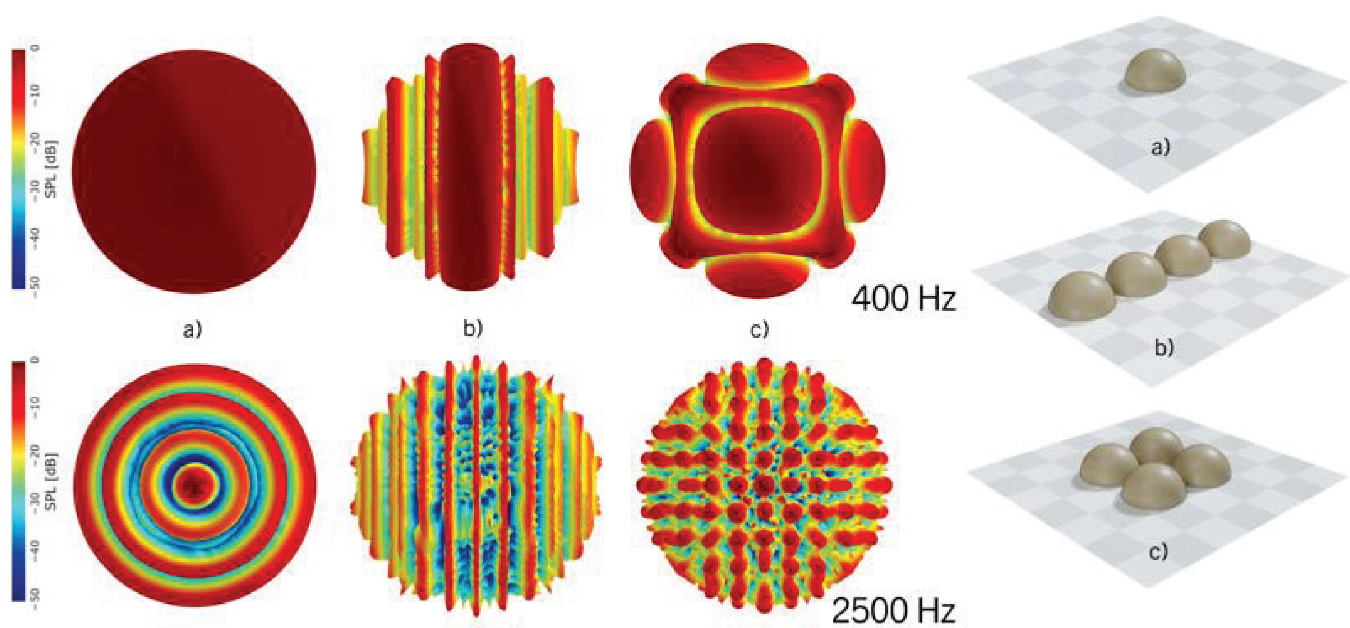

Figure 2. Comparison of the normal incidence polar response of a single hemisphere (a), a linear (b), and a square (c) array of 4 hemisphere samples.

constructive interference equation in Figure 3, we can see that at 2500 Hz the wavelength is smaller than at 400 Hz, thus allowing a larger number of diffraction orders, m, before $\sin\alpha_d$ exceeds unity. The increased number of diffraction orders is evident. The hemisphere (a) exhibits concentric rings, the linear array (b) exhibits parallel linear grating lobes, and the square array exhibits orthogonal grating lobes.

$$\sin\alpha_d = \frac{m\lambda}{w} - \sin\alpha_i$$

Figure 3. Constructive interference equation.

In Figure 4, we show the normalized diffusion coefficients for the three samples, again demonstrating how grating lobes, which arise from periodic arrays, degrade the diffusion coefficient. Later, in the Virtual Education Lab, we will describe how RPG solved this problem by optimizing asymmetric diffusors, which can be modulated using optimal binary arrays to form a larger aperiodic array with minimal grating lobes and optimal diffusion coefficients.

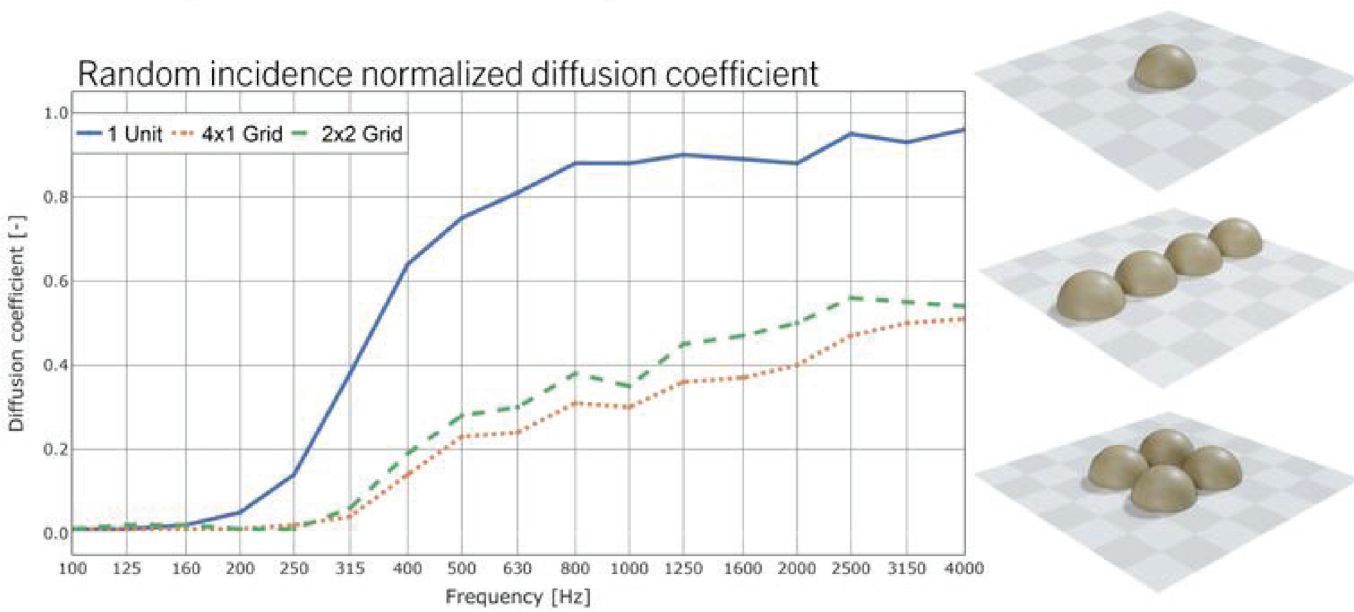

Figure 4. Normalized diffusion coefficients for 1, a 4x1 linear array, and a 2x2 grid of hemispheres.

Peter D'Antonio
Dr. Peter D'Antonio
Director of Research
Acoustical Research Center

ARC
ACOUSTICAL RESEARCH CENTER